CHEMISTRY
A EUROPEAN JOURNAL

DOI: 10.1002/chem.200701264

Metal-Ion-Dependent Biological Properties of a Chelator-Derived Somatostatin Analogue for Tumour Targeting

Axel Heppeler,[a] João P. André,[b] Ingeborg Buschmann,[a] Xuejuan Wang,[a] Jean-Claude Reubi,[c] Michael Hennig,[d] Thomas A. Kaden,[e] and Helmut R. Maecke*[a]

Abstract: Somatostatin-based radioligands have been shown to have sensitive imaging properties for neuroendocrine tumours and their metastases. The potential of [^{55}Co(dotatoc)] (dotatoc = 4,7,10-tricarboxymethyl-1,4,7,10-tetraazacyclododecane-1-ylacetyl-D-Phe-(Cys-Tyr-D-Trp-Lys-Thr-Cys)-threoninol (disulfide bond)) as a new radiopharmaceutical agent for PET has been evaluated. ^{57}Co was used as a surrogate of the positron emitter ^{55}Co and the pharmacokinetics of [^{57}Co(dotatoc)] were investigated by using two nude mouse models. The somatostatin receptor subtype (sst1–sst5) affinity profile of [^{nat}Co(dotatoc)] on membranes transfected with human somatostatin receptor subtypes was assessed by using autoradiographic methods. These studies revealed that [^{57}Co(dotatoc)] is an sst2-specific radiopeptide which presents the highest affinity ever found for the sst2 receptor subtype. The rate of internalisation into the AR4-2J cell line also was the highest found for any somatostatin-based radiopeptide. Biodistribution studies, performed in nude mice bearing an AR4-2J tumour or a transfected HEK-sst2 cell-based tumour, showed high and specific uptake in the tumour and in other sst-receptor-expressing tissues, which reflects the high receptor binding affinity and the high rate of internalisation. The pharmacologic differences between [^{57}Co(dotatoc)] and [^{67}Ga(dotatoc)] are discussed in terms of the structural parameters found for the chelate models $[Co^{II}(dota)]^{2-}$ and $[Ga^{III}(dota)]^{-}$ whose X-ray structures have been determined. Both chelates show six-fold coordination in pseudo-octahedral arrangements.

Keywords: antitumor agents · cobalt · positron emission tomography · radiopharmaceuticals · somatostatin

Introduction

The use of radionuclides in medical fields such as molecular imaging and targeted radionuclide therapy is rapidly expanding.[1,2] Radiolabelled bioactive peptides are currently being employed in tumour targeting in both positron emission tomography (PET) and single photon emission computed tomography (SPECT).[3–9] PET is an imaging modality that has the advantage of high spatial resolution, high sensitivity and the potential for quantification. For these reasons it is considered to be one of the most powerful tools for molecular imaging. Bioactive peptides labelled with metallic-particle-emitting isotopes, such as $^{90}Y^{III}$ or $^{177}Lu^{III}$, allow peptide receptor-mediated radionuclide therapy (PRMRT).[10]

The first regulatory peptides developed for radiopharmaceutical applications were somatostatin analogues, which are employed in the diagnosis of somatostatin receptor-positive tumours when modified with the chelator diethylenetriaminepentaacetic acid (DTPA) and labelled with the γ emitter ^{111}In.[11]

[a] Dr. A. Heppeler,[+] Dr. I. Buschmann, Dr. X. Wang, Prof. H. R. Maecke
Division of Radiological Chemistry
University Hospital of Basel, 4031 Basel (Switzerland)
Fax: (+41) 61-265-4699
E-mail: hmaecke@uhbs.ch

[b] Prof. J. P. André[+]
Centro de Química, Campus de Gualtar, Universidade do Minho
4710-057 Braga (Portugal)

[c] Prof. J.-C. Reubi
Division of Cell Biology and Experimental Cancer Research
Institute of Pathology, University of Berne
Murtenstrasse 31, 3010 Berne (Switzerland)

[d] Dr. M. Hennig
F. Hoffman-La Roche Ltd
Pharma Research, X-ray Crystallography
CH-4070 Basel (Switzerland)

[e] Prof. T. A. Kaden
Institute of Inorganic Chemistry, University of Basel
Spitalstrasse 51, 4056 Basel (Switzerland)

[+] These two authors contributed equally to the manuscript.

Somatostatin is a tetradecapeptide produced by neuroendocrine, inflammatory and immune cells and is thought to be an important physiological regulator of numerous functions. Its action is mediated by five receptor subtypes (sst1–sst5) that belong to the G-protein-coupled receptor family. All subtype receptors are overexpressed to some degree in different tumours, often concomitantly on the same cell.[12] By far the most important is the overexpression of receptor subtype 2. It is therefore pertinent to search for somatostatin analogues with improved affinity to sst2.

We have developed [DOTA^0,Tyr^3]-octreotide (DOTATOC, Scheme 1), a somatostatin analogue derived from 1,4,7,10-tetraazacyclododecane-*N*,*N*′,*N*″,*N*‴-tetraacetic acid (DOTA),[13] which has been successfully labelled with radiometals and proven to be useful in different areas of diagnostic and therapeutic nuclear oncology.[14] In particular the $^{68}Ga^{III}$-labelled peptide is currently being used in several European centres to afford very sensitive images of a variety of human tumours and shows an improved diagnostic accuracy, which is superior to other radiological imaging modalities, such as [^{111}In(dotatoc)].[15] [^{68}Ga(dotatoc)] shows an approximately five-fold higher binding affinity towards sst2 than [^{111}In/^{90}Y(dotatoc)]. In addition, it shows a higher rate of internalisation into sst2-expressing tumour cells, an approximately 2.5-fold higher tumour uptake and a significantly lower kidney uptake in animals and patients. We have previously shown that this difference in the biological behaviour of metallopeptides may be attributed to structural differences within the chelate moiety.[13,16]

A crystallographic study of the Ga^{III} and Y^{III} chelates of the model peptide DOTA-D-PheNH$_2$ (Scheme 1) showed differences in their geometries. [Ga^{III}(dota-D-PheNH$_2$)] is hexacoordinated with a pseudo-octahedral *cis* geometry and a folded macrocyclic unit, whereas the structure of [Y^{III}(dota-D-PheNH$_2$)] exhibits eight-fold coordination, which includes the amidic carboxy oxygen atom, with a somewhat distorted square-antiprismatic geometry. Distant from the pharmacophore of the molecule, this structural difference within the metal chelate leads to a five-fold higher receptor affinity and is probably also responsible for the mentioned improved biodistribution of the radiogallium-labelled peptide. This superiority could also be confirmed clinically by using [^{68}Ga(dotatoc)] in PET[17] and [^{67}Ga(dotatoc)] in SPECT.[13,18] This finding prompted us to exploit such structural features when using another positron-emitting metal, namely, $^{55}Co^{II}$ ($t_{1/2}$ = 17.5 h, β^+ (77%), EC (23%)). Although the structures of the Ga^{III}- and Co^{II}-labelled peptides are expected to be similar, the use of the longer-lived cyclotron-produced $^{55}Co^{II}$ as a PET radiometal could allow imaging at later points in time when target-to-background ratios are higher. There are reports in the literature of the use of $^{55}Co^{II}$ as a PET radiometal in medical fields that range from cerebrovascular diseases[19–21] to studies of human lymphocyte distribution[22] and [^{55}Co(edta)]-based quantitative imaging of the kidneys.[23]

In this work we used $^{57}Co^{II}$ ($t_{1/2}$ = 270 d, E_γ = 122 keV (86%), 136 keV (10%)) as a surrogate of $^{55}Co^{II}$ to study the biodistribution of [^{57}Co(dotatoc)] in two mouse tumour models and also to compare its receptor binding affinity and subtype specificity with those of [$^{67/68}$Ga(dotatoc)] and [^{90}Y-(dotatoc)]. In addition, X-ray studies of [Co^{II}(dota)]$^{2-}$ and [Ga^{III}(dota)]$^-$, two model chelates with relevance to the monoamide structures of the peptide derivatives, were performed with the aim of understanding the differences and similarities in the biological behaviour of the different radiometal-labelled peptides.

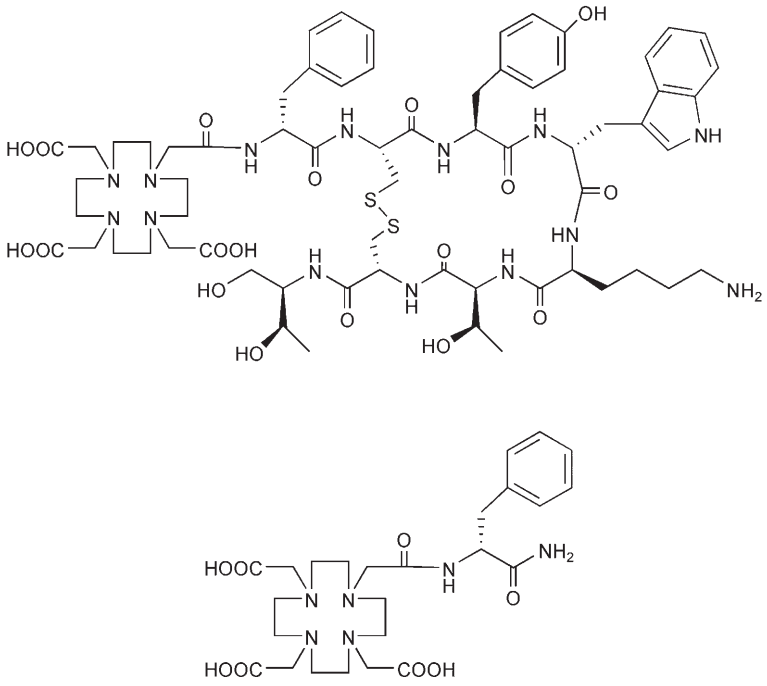

Scheme 1. Structural formulae of [DOTA^0,Tyr^3]-octreotide (DOTATOC) (above) and DOTA-D-PheNH$_2$ (below).

Results and Discussion

Synthesis, labelling and stability: The preparation of DOTATOC involved the coupling of the monoreactive DOTA(*t*Bu)$_3$ prochelator to the solid-phase-assembled, side-chain-protected peptide, as described by Ginj et al.[24] The model DOTA-peptide, DOTA-D-PheNH$_2$, was synthesised in a similar way. DOTATOC was labelled with $^{57}Co^{II}$ in acetate buffer (pH 5) by heating (95 °C, 30 min); the labelling yield was >99.5% with a specific activity of 5 mCi μmol^{-1}. [Co^{II}(dota-D-PheNH$_2$)]$^-$, [Co^{II}(dota)]$^{2-}$ and [Ga^{III}(dota)]$^-$ were prepared by

adding the ligand and metal chloride or nitrate in water and heating (95 °C, 30 min). Slow evaporation of aqueous solutions of $[Co^{II}(dota)]^{2-}$ and $[Ga^{III}(dota)]^{-}$ afforded single crystals suitable for X-ray analysis.

To understand the pharmacologic differences between [^{67}Ga(dotatoc)] and [^{57}Co(dotatoc)], we carried out NMR experiments to establish the oxidation state of the cobalt atom in the model chelates and in [^{57}Co(dotatoc)]. Labelling and complexation reactions were performed at elevated temperatures and in aerated solution, which may cause autoxidation of Co^{II}. Cobalt occurs naturally as the mononuclear isotope ^{59}Co, which has a nuclear spin $I=^{7}/_{2}$, a relatively large nuclear quadrupole moment and its chemical shifts in different chemical environments span a range of 18000 ppm. In contrast to Co^{III}, the Co^{II} ion (d^7) is paramagnetic and its complexes are therefore beyond the scope of ^{59}Co NMR spectroscopy investigations.

We performed a ^{59}Co NMR spectroscopy analysis of the model chelate $[Co^{II}(dota\text{-}D\text{-}PheNH_2)]$ and established the absence of a ^{59}Co NMR spectroscopy signal in a wide spectral window in aqueous solution. This is consistent with a +2 oxidation state. In an octahedral environment, divalent cobalt may be found in two different electronic states: a low-spin state $t_{2g}^{6}e_g^{1}$ with one unpaired electron ($S=^{1}/_{2}$) and a high-spin state $t_{2g}^{5}e_g^{2}$ with three unpaired electrons ($S=^{3}/_{2}$). The colour of the chelate is consistent with a high-spin octahedral species, typically pale-red or purple. Another strong indication for the high-spin state comes from the X-ray structure. Low-spin octahedral Co^{II} complexes undergo Jahn–Teller distortion. In $[Co(dotaH_2)]$ the equatorial Co–N bond length (2.171 Å) differs very little from that of the axial (2.203 Å). This is in contrast with the Jahn–Teller distorted [Cu(dota)] (Cu–N_{eq} = 2.107 Å, Cu–N_{ax} = 2.318 Å).

Temperature-dependent ^{1}H NMR spectroscopy studies of [Co(dota)] and $[Co(dota\text{-}D\text{-}PheNH_2)]$ over a large spectral window revealed that the number of signals and their width can vary significantly, which reflects a combination of paramagnetic shift and exchange effects, consistent with a high-spin state for the Co^{II} ion.

Our results demonstrate that dioxygen does not oxidise these polyamine polycarboxylate cobalt chelates despite the fact that the experiments were carried out in aerated solutions. This result is in accordance with earlier reports that tertiary amine ligands stabilise low-valent transition-metal ions, in particular the Co^{II} ion.[25,26]

The thermodynamic stability of $[Co^{II}(dotatoc)]$ was estimated by assessing the thermodynamic stability of the model chelate $[Co^{II}(dota\text{-}D\text{-}Phe\text{-}NH_2)]^{-}$. For this purpose, we performed complexation competition experiments by using $^{57}Co^{II}$ as a radiotracer and DOTA as an auxiliary competing ligand. Integration of the HPLC-radiochromatographic peaks that corresponded to $[^{57/59}Co(dota)]^{2-}$ and $[^{57/59}Co^{II}(dota\text{-}D\text{-}Phe\text{-}NH_2)]^{-}$ (Figure 1) remained unchanged after equilibration and allowed the conditional stability constant of $[Co^{II}(dota\text{-}D\text{-}Phe\text{-}NH_2)]^{-}$ to be estimated at different pH values.

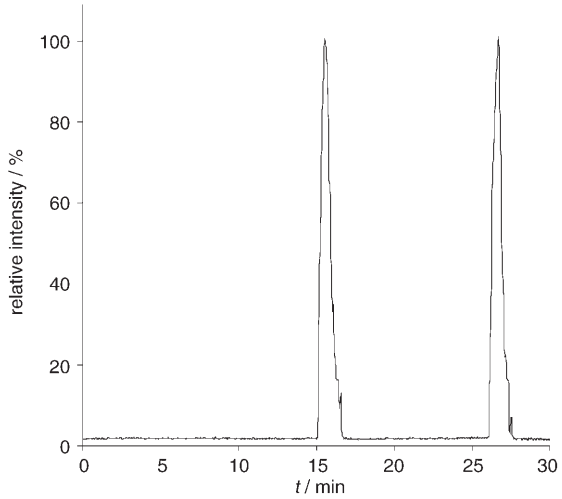

Figure 1. Typical HPLC-radiochromatogram of a 1:1:1 mixture of $^{57,59}CoCl_2$/DOTA/DOTA-D-$PheNH_2$ (0.1 M NaOAc, pH 5.0) after incubation for 9 days at room temperature [^{57,59}Co]-DOTA (left peak); [^{57,59}Co]-DOTA-D-$PheNH_2$ (right peak).

This method requires knowledge of the stability constant of $[Co^{II}(dota)]^{2-}$ ($\log K_{[Co(dota)]}=19.9$) and the protonation constants of both ligands. By using the relationships given in Equations (1), (2) and (3), in which K_1, K_2 and K_n are the protonation constants of the free ligand, we were able to estimate the thermodynamic stability constant of $[Co^{II}(dota\text{-}D\text{-}PheNH_2)]^{-}$ to be $\log K_{ML}=19.6$. This value shows that the model peptide chelate does not undergo a significant loss of thermodynamic stability in comparison to that of $[Co^{II}(dota)]^{2-}$.

$$K_{cond} = \alpha K_{ML} \quad (1)$$

$$\alpha^{-1} = (1 + K_1[H^+] + K_1K_2[H^+]^2 + \cdots + K_n[H^+]^n \quad (2)$$

$$K_{rel} = \frac{[ML_2][L_1]_t}{[ML_1][L_2]_t} = \frac{K_{ML_2}\alpha_{L_2}}{K_{ML_1}\alpha_{L_1}} \quad (3)$$

Potentiometry allowed the protonation constants (pK_as) of DOTA and DOTA-D-$PheNH_2$ to be obtained: DOTA: $pK_1=12.32(6)$, $pK_2=9.73(1)$, $pK_3=4.60(1)$, $pK_4=4.06(2)$ and $pK_5=2.08(9)$; DOTA-D-$PheNH_2$: $pK_1=11.63(14)$, $pK_2=9.28(5)$, $pK_3=4.18(14)$, $pK_4=2.14(16)$ and $pK_5<2$ ($\mu=0.5$ M tetramethylammonium nitrate, 25 °C). The lower protonation constants of DOTA-D-$PheNH_2$, in comparison with those of DOTA, arise from the difference in charge between the two chelators.

The kinetic stability of [^{57}Co(dotatoc)] with regard to *trans*-chelation was evaluated in the presence of a 10^4-fold excess of DTPA (acetate buffer, pH 5.0). The chemical inertness of the radiometal-labelled peptide was also studied by measuring the isotope exchange rate in the presence of a 10^4-fold excess of free $^{59}Co^{II}$. The results showed a high stability of [^{57}Co(dotatoc)] over a time interval of seven days (>98% intact radiopeptide).

In human serum the iron-transport protein transferrin can bind with high affinity to many metal ions, which include Co^{II}.[27] In this respect it is important to evaluate the kinetic stability of radiometal-labelled peptides under physiological conditions. For this purpose, we measured the rate of $^{57}Co^{II}$ transfer from [^{57}Co(dotatoc)] in human blood serum.[28] The approximate transfer half-life is 800 h, which compares with a value of $t_{1/2} = 1250$ h for [^{67}Ga(dotatoc)].[13]

Receptor binding assays: In Table 1 the IC_{50} values of [Co^{II}-(dotatoc)] are compared with those of other somatostatin-based metallopeptides for the five somatostatin receptor subtypes (sst1–sst5). Somatostatin 28 (SS28) was the control peptide. These values were obtained by performing a competition experiment with the cold $^{59}Co^{II}$-labelled peptide and the universal somatostatin radioligand ^{125}I-[Leu^8,D-Trp^{22},Tyr^{25}]-SS28 on cell membranes that express the different receptor subtypes. [Co^{II}(dotatoc)] exhibits around a six-fold higher affinity towards sst2 than SS28, whereas [Ga^{III}-(dotatoc)] is equipotent and [Y^{III}(dotatoc)] has a four-fold lower affinity towards sst2 than SS28. [Co^{II}(dotatoc)] shows the highest sst2 affinity of any somatostatin-based metallopeptide found so far.[12] Additionally, [Co^{II}(dotatoc)] shows a higher affinity towards sst4 than the other two metallopeptides, but a distinctly lower affinity towards sst5.

Table 1. Affinity profiles (IC_{50}) for human sst1–sst5 receptors for different somatostatin analogues.

Compound	sst1	sst2	sst3	sst4	sst5
SS-28[a]	5.2±0.3(19)	2.7±0.38(19)	7.7±0.9(15)	5.6±0.4(19)	4.0±0.3(19)
octreotide[a]	>10000(5)	2.0±0.7(5)	187±55(3)	>1000(4)	22±6(5)
[Y^{III}(dotatoc)][a]	>10000(4)	11±1.7(6)	389±135(5)	>10000(5)	114±29(5)
[Co^{II}(dotatoc)]	>10000(5)	0.44±0.11(5)	>1000(5)	610±258(4)	440±132(5)
[Ga^{III}(dotatoc)][a]	>10000(6)	2.5±0.5(7)	613±140(7)	>1000(6)	73±21(6)

[a] Data from Reubi et al.[12]

Internalisation and efflux: The specific internalisation of [^{57}Co(dotatoc)] was evaluated by using AR4-2J rat pancreatic tumour cells, which exclusively express sst2. The radiometal-labelled peptide showed a time-dependent uptake with a very high and specific internalisation rate, as shown in Figure 2 (left *y* axis and lower *x* axis).

After 6 h [^{57}Co(dotatoc)] showed almost 50% specific internalisation in 10^6 cells, which is the highest internalisation rate ever found for a somatostatin derivative. In the same cell line, [^{67}Ga(dotatoc)] showed an uptake of (16.5±1)% at 4 h p.i.,[29] [^{57}Co(dotatoc)] internalised about 30% at 4 h p.i., whereas [^{111}In(dotatoc)] internalised (11.5±0.7)% of the total amount of radiopeptide added to 10^6 cells. To evaluate the retention of the radiometal-labelled peptide in the tumour cells, externalisation experiments were also performed in AR4-2J tumour cells. Cells were preloaded with [^{57}Co(dotatoc)] for 2 h at 37 °C. To remove the receptor-bound radiometal-labelled peptide an acid wash was carried out twice with 0.1 M glycine buffer (pH 2.8, 10 min, on ice). Afterwards, externalisation of [^{57}Co(dotatoc)] was monitored at 30, 60, 120 and 240 min at 37 °C, as shown in Figure 2 (right *y* axis and upper *x* axis). The externalisation results also showed a time-dependence: the radiometal-labelled peptide presented around 40% efflux from the cells within 4 h.

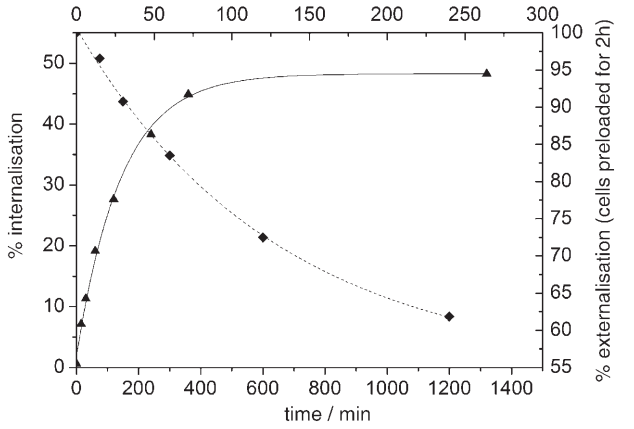

Figure 2. Internalisation (▲; scales on the left and bottom) and externalisation (◆; scales on the right and top) of [^{57}Co(dotatoc)] in rat pancreatic AR4-2J cells.

Biodistribution in tumour-bearing mice: For comparative reasons pharmacokinetic studies were performed in two mouse models (nude mice bearing the AR4-2J or HEK-sst2 tumour).[30,31] The results are given in Tables 2 and 3 and in Figure 3 as a percentage of injected activity per gram of tissue (% IA g^{-1}).

The radiometal-labelled peptide was cleared rapidly from the circulation, as demonstrated by the measurement of blood samples taken at 4, 24 and 48 h p.i. (AR4-2J) or 0.5, 1 and 4 h p.i. (HEK-sst2).

Table 2. Biodistribution of [^{57}Co(dotatoc)] in a nude mouse tumour-bearing (AR4-2J) animal model (4, 24 and 48 h p.i.).

Organ	4 h unblocked	4 h blocked	24 h	48 h
blood	0.03±0.01	0.06±0.03	0.01±0.00	0.01±0.00
pancreas	2.81±0.60	0.62±0.31	0.25±0.05	0.11±0.04
small intestine	0.69±0.34	0.27±0.11	0.21±0.02	0.08±0.02
spleen	0.11±0.22	0.12±0.04	0.07±0.02	0.03±0.00
liver	0.20±0.02	0.39±0.13	0.07±0.02	0.07±0.03
stomach	5.75±0.80	1.65±0.54	2.56±0.26	1.37±0.33
adrenals	2.33±0.54	0.75±0.15	2.20±0.43	1.33±0.41
kidneys	9.11±2.24	22.88±6.86	1.24±0.38	1.38±0.65
lung	0.34±0.06	0.41±0.15	0.06±0.03	0.05±0.02
heart	0.06±0.01	0.07±0.02	0.03±0.01	0.02±0.00
tumour	22.81±2.88	8.52±1.71	2.08±0.41	0.70±0.25
Tumour/ non-tumour ratios				
tumour/blood	760		208	70
tumour/liver	114		397	10
tumour/kidney	2.5		2.01	0.51

Table 3. Biodistribution of [^{57}Co(dotatoc)] in a nude mouse model (HEK-sstr2).

Organ	0.5 h	1 h	4 h	4 h blocking
blood	1.56 ± 0.16	0.48 ± 0.23	0.13 ± 0.02	0.12 ± 0.06
heart	0.84 ± 0.02	0.32 ± 0.03	0.19 ± 0.01	0.07 ± 0.02
liver	1.24 ± 0.05	0.69 ± 0.01	0.40 ± 0.04	0.83 ± 0.11
spleen	0.96 ± 0.22	0.67 ± 0.15	0.34 ± 0.04	0.36 ± 0.18
lung	2.29 ± 0.17	6.37 ± 2.74	1.24 ± 1.05	0.29 ± 0.06
kidneys	16.80 ± 2.20	12.15 ± 2.14	6.48 ± 0.62	8.81 ± 0.73
stomach	21.13 ± 9.09	17.10 ± 0.96	8.24 ± 1.29	0.55 ± 0.47
intestine	1.88 ± 0.05	2.18 ± 0.63	1.07 ± 0.20	0.21 ± 0.21
adrenals	2.78 ± 0.38	1.35 ± 0.08	1.58 ± 0.49	0.18 ± 0.14
pancreas	28.86 ± 0.47	15.36 ± 0.54	5.44 ± 2.13	0.34 ± 0.37
pituitary	5.80 ± 2.90	9.47 ± 1.93	4.56 ± 2.86	0.25 ± 0.09
muscle	0.82 ± 0.70	0.16 ± 0.03	0.07 ± 0.03	0.19 ± 0.29
tumour	28.35 ± 2.46	28.97 ± 3.85	34.91 ± 0.23	5.15 ± 0.79
Tumour/ non-tumour ratios				
tumour/blood	18	60	278	
tumour/liver	23	42	86	
tumour/kidney	1.7	2.4	5.4	

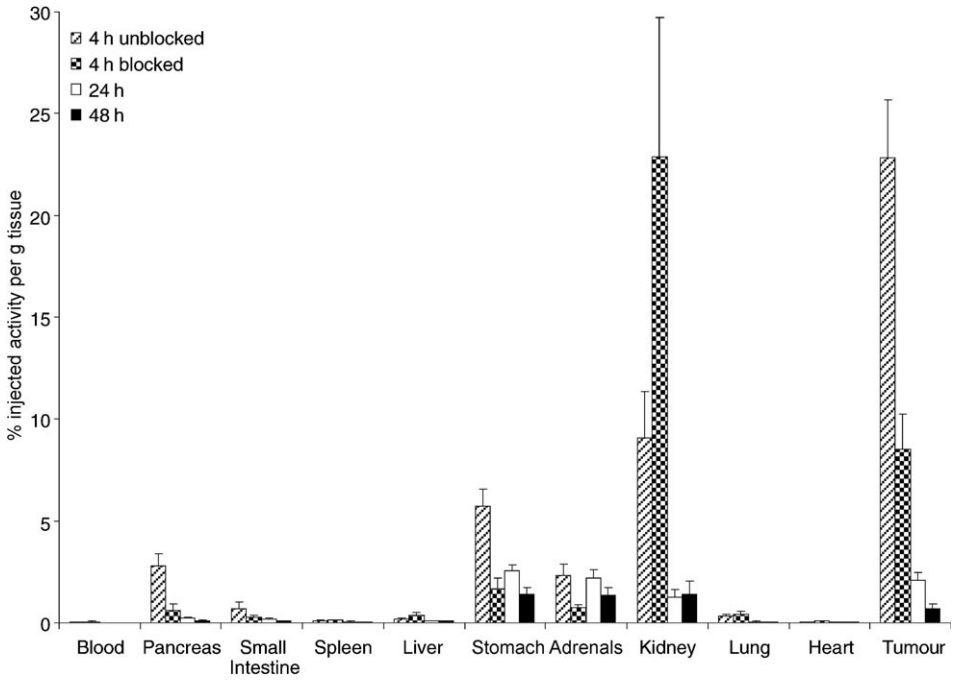

Figure 3. Biodistribution of [^{57}Co(dotatoc)] in nude mice with a tumour (% IA g^{-1}: % injected activity per gram).

Less than 0.15 % IA g^{-1} remained in the blood after 4 h. The clearance from all somatostatin receptor-negative tissues, which included the kidneys, was also fast. Unexpectedly, the tumour uptake in the AR4-2J tumour also decreased between 4 and 24 h by > 90 %. This has never been observed before in any somatostatin-based radiopeptide, which usually show biological half-lives of ≥ 24 h in tumours of this tumour model.[30] The highest tissue activity was found in the kidneys, which demonstrates the renal excretion of the radiopharmaceutical. At all time points the uptake in other organs was considerably lower except for the stomach, which is known to contain somatostatin receptors. Some uptake could be seen in the pancreas and the adrenals as well, which was expected because these two organs express somatostatin receptors. The pancreas shows a good clearance after 24 h, whereas the uptake in the adrenals stays relatively high (60 % of the 4 h value after 48 h).

A high radioligand accumulation was measured in the tumours 4 h after injection. When the receptors were blocked by a simultaneous injection of octreotide, the accumulation of radioactivity in the tumour was significantly reduced by 63 %. A higher reduction could be seen in the stomach (71 %), the pancreas (88 %) and the adrenals (68 %). Upon blocking, the accumulation in the kidneys increased by a factor of 2.5.

In all non-tumour and non-receptor-specific tissues a rapid clearance of the radiopharmaceutical was observed; this is also true for the kidneys (after 48 h 15 % of the activity of the 4 h value is found in this organ).

The HEK-sst2 model was used to study the pharmacokinetics after shorter time intervals for comparative reasons. The general picture is similar to the other tumour model. The tumour uptake was very high, doubling the value obtained by using another potent sst2-selective radiopeptide, [^{111}In(dtpa-tate)] (IC_{50} = 1.3 nM), at 4 h p.i.[31] Blocking was performed by co-injection of 100 μg [DOTA,-Tyr^3,Thr^8]octreotide (DOTA-TATE) and was more efficient than blocking with 50 μg octreotide in the AR4-2J mouse model. The unspecific level was lowered to 14.7 % in the tumour, 6.3 % in the pancreas and 5.5 % in the pituitary. The tumour uptake was persistent, even increasing, in the first 4 h, whereas the initial high pancreas uptake was washed out relatively quickly. The tumour/blood, tumour/liver and tumour/kidney ratios increased considerably during the first 4 h and a value of 5.4 has never before been observed in this or any other similar tumour model that uses a somatostatin-based radiometallopeptide.

Coordination chemical aspects: It is of major importance to understand why the radiometal ion influences the receptor binding affinity and the tumour uptake. With regard to this we crystallised two model chelates, [$Co^{II}(H_2dota)$] and [$Ga^{III}(dota)]^-$, which correspond to the metal chelate moiet-

ies of [Co^{II}(dotatoc)] and [Ga^{III}(dotatoc)], respectively, and determined their X-ray structures. Both chelates crystallise as diprotonated species. ORTEP representations of the chelates are shown in Figures 4 and 5 and the crystallographic data are summarised in Table 4.

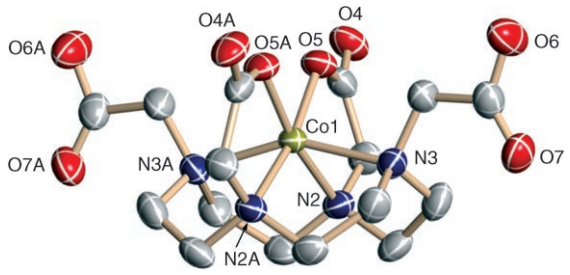

Figure 4. ORTEP plot of the crystal structure of $[Co^{II}(dota)]^{2-}$ (thermal ellipsoids at the 50% probability level). Selected bond lengths [Å] and angles [°]: Co1–N2 2.271(6), Co1–N2 2.271(6), Co1–N3 2.203(6), Co1–N3 2.203(6), Co1–O5 2.038(5), Co1–O5 2.038(5); N2-Co1-N2 108.1(3), N3-Co1-N3 154.0(3), O5-Co1-O5 90.7(3).

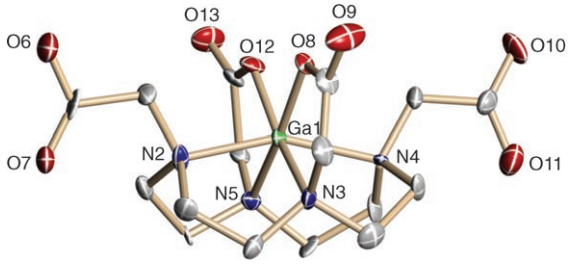

Figure 5. ORTEP plot of the crystal structure of $[Ga^{III}(dota)]^{-}$ (thermal ellipsoids at the 50% probability level). Selected bond lengths [Å] and angles [°]: Ga1–N3 2.105(9), Ga1–N5 2.116(9), Ga1–N2 2.116(10), Ga1–N4 2.187(10), Ga1–O8 1.940(7), Ga1–O12 1.913(8); N3-Ga1-N5 109.0(2), O12-Ga1-O8 82.39(13), N2-Ga1-N4 157.1(2).

Table 4. Crystallographic data for $[Co^{II}(dota)]^{2-}$ and $[Ga^{III}(dota)]^{-}$ chelates.

	$[Co^{II}(H_2dota)]$	$[Ga^{III}(H_2dota)]^{+}Cl^{-}$
formula	$C_{16}H_{26}CoN_4O_8$	$C_{16}H_{26}ClGaN_4O_8{\cdot}5H_2O$
f_w	461.34	597.65
crystal size [mm]	0.6×0.6×0.4	0.5×0.5×0.5
space group	*Pccn*	*Cc*
crystal system	orthorhombic	monoclinic
a [Å]	15.225(3)	15.171(90)
b [Å]	9.3920(19)	14.962(94)
c [Å]	13.065(3)	10.068(90)
V [$Å^{-3}$]	1868.2(6)	2279.5
Z	4	4
ρ_{calcd} [$g\,cm^{-3}$]	1.640	1.706
T [K]	183(2)	183(2)
μ [mm^{-1}]	0.974	1.400
λ [Å]	0.71073 ($Mo_{K\alpha}$)	0.71073 ($Cu_{K\alpha}$)

The structures of the $[Co^{II}(dota)]$ and $[Ga^{III}(dota)]$ chelates are very similar, showing six-coordination and a pseudooctahedral geometry. Two macrocyclic ring nitrogen atoms and two *trans*-arranged carboxylate oxygen atoms are bound axially, whereas the remaining two ring nitrogen atoms form equatorial bonds to the metals. Deviation from the octahedron is seen in the equatorial N-M-N bond angles of 154 and 157° for $[Co^{II}(H_2dota)]$ and $[Ga^{III}(H_2dota)]^{+}$, respectively (180° is expected in a regular octahedron). Table 5 shows some selected bond lengths, angles and planes

Table 5. Selected average bond lengths [Å], angles [°] and planes for the $[Co^{II}(dota)]^{2-}$ and $[Ga^{III}(dota)]^{-}$ chelates.

		$[Co^{II}(H_2dota)]$	$[Ga^{III}(H_2dota)]^{+}$
CN[a]		6	6
ring configuration		2424	2424
M–N [Å]	eq	2.171(6)	2.111(8)
	ax	2.203(6)	2.152(50)
N-M-N [°]	eq	154.0(3)	157.1(2)
	ax	108.1(3)	109.0(2)
O-M-O [°]	eq	90.7(3)	82.39(2)
M–O [Å]	eq	2.038(5)	1.927(19)
D_{N2O2}[b] [Å]		0.037	0.068
R_{N2O2}[b] [Å]		0.08	0.005

[a] CN is the coordination number of the metal ion. [b] D_{N2O2} is the distance to the plane. R_{N2O2} is the distance of the defining atoms to the best plane (P_{N2O2}).

for both chelates. The two structures are almost identical and similar to the corresponding structure of $[Ga^{III}$(dota-D-PheNH$_2$)],[13] which shows the relevance of the structures to the monoamide peptide derivatives. In both structures, as in $[Ga^{III}$(dota-D-PheNH$_2$)], the macrocyclic unit adopts a 2424 conformation. The somewhat smaller bond lengths in $[Ga^{III}(H_2dota)]^{+}$, relative to those in $[Co^{II}(H_2dota)]$, are compatible with a metallic centre of higher charge density (ionic radius of Ga^{3+} = 62 pm; ionic radius of $Co^{2+}{}_{high\ spin}$ = 73.5 pm).

As in $[Ga^{III}$(dota-D-PheNH$_2$)],[13] $[Ga^{III}(H_2dota)]^{+}$ and $[Co^{II}(H_2dota)]$ only show the coordination of two acetate groups, whereas the remaining two are free and one of them will always be used when the chelator is coupled to a biomolecule to form an amide bond. The similar structural features of $[Co^{II}(H_2dota)]$ and $[Ga^{III}(H_2dota)]^{+}$ allow us to assume that [^{57}Co(dotatoc)] and [^{67}Ga(dotatoc)] might also have similar structures and consequently one would expect the two radiopeptides to have similar biological behaviour. The fact that in both radiopeptides one carboxylate group is free and deprotonated at physiological pH contributes to their fast and efficient clearance through the kidneys. Despite the likely structural similarities of [^{57}Co(dotatoc)] and [^{67}Ga(dotatoc)], the two radiopeptides show remarkably different biological behaviour, which we have tended to assign to the different charge density of the metal ions.

Conclusion

[^{57}Co(dotatoc)] and [^{67}Ga(dotatoc)] are two radiopharmaceuticals that, despite their structural similarities (as shown by the X-ray structures of the model chelates $[Co^{II}(H_2dota)]$

and [$Ga^{III}(H_2dota)]^+$), display different biological behaviour. [^{57}Co(dotatoc)] presents the highest affinity for the sst2 subtype receptor of any radiometal-labelled somatostatin derivative. The improved receptor binding affinity is reflected in a high and specific tumour uptake and a high rate of internalisation. [^{57}Co(dotatoc)] has a relatively short tumour residence time in the AR4-2J animal model. This may not be a disadvantage if there is a similar response in humans because it would lead to a low patient dose. In addition, its tumour-to-kidney ratio is one of the highest of any radiopeptide of the somatostatin analogues.

Cobalt in [^{57}Co(dotatoc)] is present in the +2 oxidation state, as demonstrated in aqueous solutions of [$Co^{II}(H_2dota)$] and [Co^{II}(dota-D-PheNH$_2$)]$^-$, and the coordination geometry of the Co^{II} ion is a somewhat distorted octahedron.

This work illustrates how the physical features (size, charge) of the radiometal strongly influence receptor affinity, biodistribution and the pharmacokinetics of radiometal-labelled peptides. Our results encourage further animal and possibly clinical studies to evaluate the full potential of [^{55}Co(dotatoc)] as a PET agent.

Experimental Section

Chemicals and analysis: All chemicals were obtained from commercial sources and used without further purification. DOTA was a gift from Guerbet (France). $^{57}CoCl_2$ was purchased from Isotope Products Laboratories (Burbank, CA USA). Sephadex G-50 (Pharmacia) was used for gel chromatography. Electrospray ionisation (ESI) was carried out by using a Finnigan SSQ 7000 spectrometer. Analytical and semipreparative HPLC was performed by using a Hewlett-Packard 1050 HPLC system with a multiwavelength detector and a flow-through Berthold LB 506 C1 γ detector. Quantitative γ counting was performed with a COBRA 5003 γ system well-counter from Packard Instrument Company. ^{1}H and ^{13}C NMR spectroscopies were performed by using either a Varian VXR 400 spectrometer at 400/101 MHz or a Varian Unity 500 spectrometer at 500/126 MHz. Chemical shifts are reported relative to TMS. ^{59}Co NMR spectroscopy was performed by using a Bruker AV400 spectrometer at 94.939 MHz; 0.1 M $K_3[Co(CN)_6]$ in D_2O was used as the external reference and the presence of signals was checked between +15000 and −1000 ppm.

Syntheses and labelling: DOTATOC and [Ga^{III}(dotatoc)] were synthesised as described previously.[13]

[^{57}Co(dotatoc)]: [^{57}Co(dotatoc)] was prepared as follows: DOTATOC (10 μg, 7 nmol) was dissolved in a sodium acetate buffer (20 μL, 0.4 M, pH 5.0). $^{57}CoCl_2$ (43 μCi) was added and the mixture heated at 95 °C for 30 min. Quality control was performed with HPLC (Nucleosil 120-C18, M&N; eluents: A = 0.1 % TFA in H_2O and B = CH_3CN; gradient: 0–5 min 100 % A, 25 min 75 % A, 30–35 min 100 % A). The labelling yield was >99.5 %; the achieved specific activity was 5 mCi μmol^{-1}, which corresponds to a peptide/^{57}Co ratio of 50:1. MS (ESI): *m/z*: 1477.3 [*M*−H]$^-$ (100 %), 1499.5 [*M*+HCOO$^-$]$^-$ (20 %), 1535.8 [*M*+CH_3COO^-]$^-$ (10 %); purity (HPLC): >97 %.

[Co^{II}(dota-D-PheNH$_2$)]$^-$: [Co^{II}(dota-D-PheNH$_2$)]$^-$ was obtained by treating DOTA-D-PheNH$_2$ (8.0 mg, 14.5 μmol) with $CoCl_2 \cdot 6H_2O$ (3.8 mg, 16 μmol) in aqueous solution (1 mL, pH 4, 95 °C, 30 min). After cooling to room temperature the pH was adjusted to 5 with 0.1 M aqueous NaOH. Evaporation to dryness afforded a purple solid in quantitative yield. ^{1}H NMR (500 MHz, 25 °C, D_2O): δ = 6.9 (br s, 2H; arom. *ortho*), 7.7 ppm (m, 2H, 1H; arom. *meta*, arom. *para*); in the 2.25–3.25 ppm range three small broad signals were detected (each one with an integration corresponding to 1H). We checked for ^{1}H NMR signals in a spectral window of +400 to −400 ppm in the temperature range of 5 to 90 °C. ^{59}Co NMR spectroscopy (94.939 MHz, 25 °C, D_2O) showed no signals in a spectral window of +15000 to −1000 ppm; MS (ESI): $C_{25}H_{36}CoN_6O_8$ (*M* = 607.5 g mol^{-1}): *m/z* (%): 608.8 (30) [*M*+H]$^+$, 630.5 (20) [*M*+Na]$^+$, 606.4 (100) [*M*−H]$^-$.

[$Co^{II}(H_2dota)$]: [$Co^{II}(H_2dota)$] was obtained by treating DOTA (50 mg, 0.12 mmol) with $CoCl_2 \cdot 6H_2O$ (28.6 mg, 0.12 mmol) in aqueous solution (5 mL, pH 4.8, 95 °C, 25 min). Slow evaporation produced light-red single crystals suitable for X-ray analysis. ^{1}H NMR (400 MHz, 25 °C, D_2O): no signals were observed; MS (ESI): $C_{16}H_{26}CoN_4O_8$ (*M* = 461.11 g mol^{-1}): *m/z* (%): 462.1 (100) [*M*+H]$^+$.

[$Ga^{III}(H_2dota)]^+Cl^-$: [$Ga^{III}(H_2dota)]^+Cl^-$ was obtained by treating DOTA (78.73 mg, 0.181 mmol) with $Ga(NO_3)_3 \cdot 9H_2O$ (91 mg, 0,217 mmol) in aqueous solution (5 mL, pH 4, 80 °C, 30 min). After cooling to room temperature, the pH was adjusted to 8 with 0.1 M aqueous NaOH. Excess Ga^{III} (in the form of hydroxide) was removed by filtration and the final pH was adjusted to 7 with 0.1 M HCl. Slow evaporation of water afforded colourless crystals suitable for X-ray diffraction. ^{1}H NMR: (400 MHz, 27 °C, D_2O): δ = 3.40 (br s, 16H, N-CH_2-CH_2-N), 3.68 ppm (br s, 8H; N-CH_2-COOD); ^{13}C NMR: (101 MHz, 27 °C, D_2O, pD = 6.9): δ = 52.52 (N-*C*H_2-*C*H_2N), 58.48 (N-*C*H_2-COOGa), 176.40 ppm (*C*OOGa); IR (KBr): ν = 3570, 3492, 2956, 2705, 2650, 2590, 1746, 1710, 1699, 1620, 1496, 1475, 1384, 1339, 1316, 1287, 1240, 1212, 1083, 1047, 925 cm^{-1}; MS (ESI): $C_{16}H_{25}GaN_4O_8$ (*M* = 471.11 g mol^{-1}): *m/z* (%): 471.1, 472.1 (6:4) (100) [*M*+H]$^+$; elemental analysis calcd (%) for $C_{16}H_{25}N_4O_8Ga \cdot HNO_3 \cdot 2H_2O$ (*M* = 570.16 g mol^{-1}): C 33.71, H 5.30, N 12.29, O 36.47; found: C 33.57, H 5.10, N 12.25, O 31.52.

Kinetic exchange: The kinetic stability of [^{57}Co(dotatoc)] upon *trans*-chelation was determined by using a 10^4-fold excess of DTPA. [^{57}Co(dotatoc)] (6 μL, 10^{-11} mol) was mixed with DTPA (10 μL, 10^{-7} mol) and 0.1 M aqueous NaOAc (484 μL, pH 5.0). The exchange rate of this solution was measured by removing aliquots (50 μL) and the exchange ratio for [^{57}Co(dotatoc)] versus [$^{57}Co^{II}$(dtpa)]$^{3-}$ was analysed by HPLC at time intervals of 4 to 24 h.

In addition, the chemical inertness of [^{57}Co(dotatoc)] was verified by measuring the isotope exchange rate of the radiocobalt-labelled peptide versus a 10^4 excess of free $^{59}Co^{II}$. The experiment was carried out by using similar concentrations of [^{57}Co(dotatoc)] and $^{59}CoCl_2$ as described above. Aliquots of 50 μL were incubated with DTPA (10^{-3} M, 10 μL) prior to HPLC analyses to enable detection of $^{57}Co^{II}$ as the [^{57}Co(dtpa)]$^{3-}$ complex.

Serum stability studies: [^{57}Co(dotatoc)] was added to fresh human blood serum (1 μCi mL^{-1}) and incubated at 37 °C in a CO_2 atmosphere (5 %). At defined times aliquots of 50 to 100 μL were taken and analysed by gel chromatography (Sephadex G50, PBS buffer 0.01 M, pH 7.4). Low- and high-molecular fractions were collected and measured with a γ counter. The amount of serum protein-bound radiopeptide was calculated by the count rates of both fractions.[32]

Thermodynamic stability and protonation constants: The thermodynamic stability constant of [Co^{II}(dota-D-PheNH$_2$)]$^-$ was estimated by competition experiments by using DOTA as a competing chelator. For this purpose, solutions that contained similar amounts of both ligands were used (0.01 M, 40 μL). $^{57/59}CoCl_2$ was added in phosphate buffer (0.01 M, pH 7.0, 20 μL). The mixture was incubated at room temperature at a controlled pH. Aliquots of 15 μL were taken at different times and analysed by HPLC equipped with a Berthold γ detector (CC 250–4 mm 120–3 C_8, M&N, eluent: A = 0.1 % TFA in H_2O, B = CH_3CN; 0–5 min 100 % A, 25–35 min 30 % B, 35 min 100 % A).

The protonation constants of DOTA and DOTA-D-Phe-NH_2 were obtained by potentiometric titration in a thermostatted cell at 25 °C under a stream of N_2 with a 0.5 M aqueous solution of tetramethylammonium hydroxide (standardised with potassium hydrogenophthalate) at an ionic strength adjusted to 0.5 M with tetramethylammonium nitrate in a Metrohm 665-Dosimat equipped with a 1 mL piston burette. Excess nitric acid was added to the ligand solutions to determine the lower protonation constants. All of the solutions were prepared with deionised water (Millipore), which was previously boiled to remove CO_2. All pH meas-

urements were carried out by using a Metrohm 645 digital pH meter equipped with a Metrohm 6.0204.100 glass electrode combined with a calomel (3 M aqueous KCl) reference electrode. The glass electrode was calibrated with pH 4.0 and 7.0 buffers at 25 °C. The pH meter/electrode system was calibrated by titrating a 3.2 mM TRIS solution with 0.5 M tetramethylammonium hydroxide at an ionic strength adjusted to 0.5 M with tetramethylammonium nitrate. The data were handled and calculated with the TITFIT program.[33]

Cell culture: AR4-2J rat pancreatic tumour cells expressing sst2 were cultured in high glucose Dulbecco's minimal essential medium (DMEM) enriched with 4 nM glutamine, 10% FBS, amino acids, vitamins and penicillin-streptomycin from BioConcept (Allschwil, Switzerland). Cells were maintained in a humidified 5% CO_2/air atmosphere at 37 °C. The viability of the cells was assessed by using trypan blue stain and counted under a microscope with a Neubauer's counting chamber.

Receptor binding assays: Cells that stably expressed human sst1, sst2, sst3, sst4 and sst5 were grown as described previously.[12] All culture reagents were supplied by Gibco and Life Technologies (Grand Island, NY). Cell membrane pellets were prepared and receptor autoradiography was performed on pellet sections (mounted on microscope slides), as described in detail previously.[12]

Complete displacement experiments were performed with the universal somatostatin radioligand ^{125}I-[Leu^8,D-Trp^{22},Tyr^{25}]-somatostatin-28 (2000 Ci mmol^{-1}; Anawa (Wangen, Switzerland)) by using increasing concentrations of the unlabelled peptide that ranged from 0.1 to 1000 nM. Experiments with somatostatin-28 were run in parallel as a control by using the same increasing concentrations. IC_{50} values (inhibitory concentration 50%) were calculated after quantification of the data by using a computer-assisted image processing system. Tissue standards (autoradiographic [^{125}I] microscales, Amersham, UK) that contained known amounts of isotopes, cross-calibrated to tissue-equivalent ligand concentrations, were used for quantification.[12] The peptide concentration was measured by UV spectroscopy ($\varepsilon_{280nm} = 6849$ L mol^{-1} cm^{-1}), according to the method developed by Reubi et al.,[12] and was based on the exact knowledge of the elemental analysis of DOTATOC.

Internalisation and efflux studies: Cells (10^6 per well) were distributed in six-well plates at 37 °C in a 5% CO_2/air atmosphere for one night in a culture medium (DMEM with 10% FBS). The medium was removed, the cells were washed and incubated for 1 h in the internalisation medium (DMEM with 1% FBS) under the same conditions as described above. Approximately 0.02 MBq per well of the radioligand (2.5 pmol per well) were added to the medium and the cells were incubated at 37 °C, 5% CO_2, with and without an excess of the peptide (1 μg) to determine non-specific internalisation. At appropriate time periods, the internalisation was stopped by removing the medium and washing the cells with ice-cold PBS. To remove the receptor-bound radioligand, an acid wash was carried out with 0.1 M glycine buffer pH 2.8 for 10 min on ice. This procedure permits a distinction to be made between membrane-bound (acid-releasable) and internalised radioligand (acid-resistant). Finally, cells were solubilised with 1 M aqueous NaOH and incubated for 10 min at 37 °C. The radioactivity of the culture medium, the receptor-bound and the internalised fractions were measured in a γ counter (Cobra II, Packard Instruments (Switzerland)).

For externalisation experiments the AR4-2J cells (10^6 per well) were incubated with radioligand (2.5 pmol per well). After 2 h of internalisation at 37 °C, 5% CO_2, the medium was removed and the cells were washed twice with cold PBS. An acid wash was performed, as described in the previous section. The internalisation medium (3 mL) was added to each well and the cells were incubated at 37 °C. At different times the external medium was collected and exchanged with fresh medium at 37 °C. Thereafter, the cells were treated with 1 M aqueous NaOH to extract the internalised radioligand. The radioactivity of the external medium and the internalised radioligand fractions was quantified in a γ counter. The recycled fraction was expressed as a percentage of the totally internalised amount per 10^6 cells.

Biodistribution studies in tumour-bearing animals: All animal experiments were performed in compliance with Swiss laws on animal protection (approval no. 789). Male nude mice (IFFACREDO (France)) were subcutaneously injected in the right abdomen with a cell suspension of a rat pancreatic cell tumour (AR4-2J, 5×10^6 cells per 50 μL). Six to seven days post-injection the tumours had grown to a size of approximately 0.5 cm in diameter. The animals were split into four groups: three batches of four animals without pretreatment for 4, 24 and 48 h biodistribution studies, and four animals which were injected with 50 μg Octreotide together with the radiopharmaceutical. Both substances, the radioligand and the Octreotide, were prepared in a 0.1% bovine serum albumin solution to prevent the substances from sticking to the syringes. For the second tumour model five-week-old female Swiss athymic nude mice were subcutaneously implanted with 10×10^6 of HEK-sst2 cells on one flank. After 10 to 12 d the mice exhibited solid palpable tumour masses of 150 to 200 mg. To study the biodistribution of [^{57}Co(dotatoc)], the radioligand (3 μCi, (120 ± 15) kBq) was injected into the tumour-bearing mice as a bolus in the tail vein. After the respective times the animals were sacrificed, a blood sample was taken, organs were removed and weighed and the radioactivity was counted.

X-ray diffraction studies: The X-ray measurements of $[Ga^{III}(dota)]^-$ and $[Co^{II}(dota)]^{2-}$ were performed by using a Nicolet P3 diffractometer with graphite-monochromated $Mo_{K\alpha}$ radiation. The crystallographic data are summarised in Table 4 and the average bond lengths, angles and planes in Table 5. The structures were solved by using Patterson methods, expanded by Fourier techniques and refined against F^2 by full-matrix least-squares methods by using the SHELX93 crystallographic software package.[34]

CCDC 616729 ($[Ga^{III}(dota)]^-$) and 616730 ($[Co^{II}(dota)]^{2-}$) contain the supplementary crystallographic data for this paper. These data can be obtained free of charge from the Cambridge Crystallographic Data Centre via www.ccdc.cam.ac.uk/data_request/cif.

Acknowledgements

This work was supported by the Swiss National Science Foundation (project no. 320000-114043). J.P.A. thanks the Foundation of Science and Technology (F.C.T.), Portugal, for the grant received during his sabbatical leave. Novartis (Basel, Switzerland) is acknowledged for the MS-ESI analysis. Kayhan Akyel is acknowledged for the ^{1}H NMR spectra. Dr. Maryse Bourdonneau (Bruker, Wissenbourg, France) is acknowledged for the ^{1}H and ^{59}Co NMR spectra. The authors thank Daniel Storch for his help in the preparation of the figures for the manuscript.

[1] P. Blower, *Dalton Trans.* **2006**, 1705–1711.
[2] S. Liu, *Chem. Soc. Rev.* **2004**, *33*, 445–461.
[3] T. M. Behr, M. Gotthardt, A. Barth, M. Behe, *Q. J. Nucl. Med.* **2001**, *28*, 1421–1429.
[4] S. M. Okarvi, *Med. Res. Rev.* **2004**, *24*, 357–397.
[5] M. Ginj, H. R. Maecke, *Met. Ions Biol. Syst.* **2004**, *42*, 109–142.
[6] J. C. Reubi, *Endocr. Rev.* **2003**, *24*, 389–427.
[7] R. E. Weiner, M. L. Thakur, *BioDrugs* **2005**, *19*, 145–163.
[8] H. R. Maecke, J. P. Andre, *Ernst Schering Res. Found. Workshop* **2007**, 215–242.
[9] J. C. Reubi, H. R. Maecke, E. P. Krenning, *J. Nucl. Med.* **2005**, *46*, 67S-75S.
[10] M. de Jong, W. A. Breeman, R. Valkema, B. F. Bernard, E. P. Krenning, *J. Nucl. Med.* **2005**, *46*, 13S–17S (Supplement 1).
[11] D. J. Kwekkeboom, E. P. Krenning, W. H. Bakker, H. Y. Oei, P. P. Kooij, S. W. Lamberts, *Eur. J. Nucl. Med.* **1993**, *20*, 283–292.
[12] J. C. Reubi, J. C. Schar, B. Waser, S. Wenger, A. Heppeler, J. S. Schmitt, H. R. Maecke, *Eur. J. Nucl. Med.* **2000**, *27*, 273–282.
[13] A. Heppeler, S. Froidevaux, H. R. Mäcke, E. Jermann, M. Béhé, P. Powell, M. Hennig, *Chem. Eur. J.* **1999**, *5*, 1016–1023.
[14] D. J. Kwekkeboom, J. Mueller-Brand, G. Paganelli, L. B. Anthony, S. Pauwels, L. K. Kvols, M. O'Dorisio, T. R. Valkema, L. Bodei, M. Chinol, H. R. Maecke, E. P. Krenning, *J. Nucl. Med.* **2005**, *46*, 62S-66S.

[15] H. R. Maecke, M. Hofmann, U. Haberkorn, *J. Nucl. Med.* **2005**, *46*, 172S-178S.
[16] M. de Jong, W. H. Bakker, E. P. Krenning, W. A. Breeman, M. E. van der Pluijm, B. F. Bernard, T. J. Visser, E. Jermann, M. Béhé, P. Powell, H. R. Maecke, *Eur. J. Nucl. Med.* **1997**, *24*, 368–371.
[17] M. Henze, A. Dimitrakopoulou-Strauss, S. Milker-Zabel, J. Schuhmacher, L. G. Strauss, J. Doll, H. R. Maecke, M. Eisenhut, J. Debus, U. Haberkorn, *J. Nucl. Med.* **2005**, *46*, 763–769.
[18] K. Zhernosekov, P. Aschoff, D. Filosofov, M. Jahn, M. Jennewein, H. J. Adrian, H. Bihl, F. Rosch, *Eur. J. Nucl. Med. Mol. Imaging* **2005**, *32*, 1129.
[19] H. M. Jansen, J. Pruim, A. M. v. d. Vliet, A. M. Paans, J. M. Hew, E. J. Franssen, B. M. de Jong, J. G. Kosterink, R. Haaxma, J. Korf, *J. Nucl. Med.* **1994**, *35*, 456–460.
[20] H. Stevens, H. M. Jansen, J. De Reuck, M. Lemmerling, K. Strijckmans, P. Goethals, I. Lemahieu, B. M. de Jong, A. T. Willemsen, J. Korf, *J. Neurol. Sci.* **1999**, *171*, 11–18.
[21] J. De Reuck, K. Paemeleire, P. Santens, K. Strijckmans, I. Lemahieu, *Clin. Neurol. Neurosurg.* **2004**, *106*, 77–81.
[22] J. Korf, L. Veenma-van der Duin, R. Brinkman-Medema, A. Niemarkt, L. F. de Leij, *J. Nucl. Med.* **1998**, *39*, 836–841.
[23] Z. Szabo, J. Xia, W. B. Mathews, P. R. Brown, *Semin. Nucl. Med.* **2006**, *36*, 36–50.
[24] M. Ginj, J. S. Schmitt, J. Chen, B. Waser, J. C. Reubi, M. de Jong, S. Schulz, H. R. Maecke, *Chem. Biol.* **2006**, *13*, 1081–1090.
[25] G. Golub, H. Cohen, D. Meyerstein, *J. Chem. Soc., Chem. Commun.* **1992**, 397–398.
[26] I. Bertini, L. Messori, G. Golub, H. Cohen, D. Meyerstein, *Inorg. Chim. Acta* **1995**, *235*, 5–8.
[27] T. A. Smith, *Bioorg. Med. Chem.* **2005**, *13*, 4576–4579.
[28] G. Ruser, W. Ritter, H. R. Maecke, *Bioconjugate Chem.* **1990**, *1*, 345–349.
[29] P. Antunes, M. Ginj, H. Zhang, B. Waser, R. P. Baum, J. C. Reubi, H. Maecke, *Eur. J. Nucl. Med. Mol. Imaging* **2007**, *34*, 982–993.
[30] S. Froidevaux, A. N. Eberle, M. Christe, L. Sumanovski, A. Heppeler, J. S. Schmitt, K. Eisenwiener, C. Beglinger, H. R. Maecke, *Int. J. Cancer* **2002**, *98*, 930–937.
[31] M. Ginj, H. Zhang, B. Waser, R. Cescato, D. Wild, X. Wang, J. Erchegyi, J. Rivier, H. R. Macke, J. C. Reubi, *Proc. Natl. Acad. Sci. U.S.A.* **2006**, *103*, 16436–16441.
[32] A. Riesen, T. Kaden, W. Ritter, H. Maecke, *J. Chem. Soc., Chem. Commun.* **1989**, 460.
[33] A. Zuberbuehler, T. Kaden, *Talanta* **1982**, *29*, 201–206.
[34] G. M. Sheldrick, *Acta Crystallogr., Sect. A* **1990**, *46*, 467–473.

Received: August 14, 2007
Published online: February 1, 2008

